PRL-TN-2012-102
Technical Note

Development of Automated Digital Optical Imagers for Photography of Vapour Cloud Releases By Rocket

by
Ravindra Pratap Singh, Duggirala Pallamraju and R. Narayanan
(Space and Atmospheric Sciences Division)

भौतिक अनुसंधान प्रयोगशाला, अहमदाबाद
Physical Research Laboratory, Ahmedabad

PRL-TN-2012-102
Technical Note

Development of Automated Digital Optical Imagers for Photography of Vapour Cloud Releases By Rocket

by
Ravindra Pratap Singh, Duggirala Pallamraju and R. Narayanan
(Space and Atmospheric Sciences Division)

भौतिक अनुसंधान प्रयोगशाला, अहमदाबाद
Physical Research Laboratory, Ahmedabad

Published by
The Dean's office, PRL.

Contents

Development of Automated Digital Optical Imagers for Photography of Vapour Cloud Releases By Rocket

Ravindra Pratap Singh, Duggirala Pallamraju and R. Narayanan

Physical Research Laboratory, Ahmedabad
(ravindra@prl.res.in)

1. Abstract: *In this report we present the technical details on the development of digital optical imagers that are capable of photography of vapour clouds released by sounding rockets. As photography of vapour clouds requires synchronous operation from different locations, it is extremely important that these imagers are automated and perform reliably. This report also presents the work carried out towards the automation of these imagers. These imaging systems are less expensive, easily portable, highly reliable, and very rugged. These are also easy to handle, install, and operate. These features make these imagers highly suitable for field operations, which are extremely essential for photography of vapour cloud releases by rockets. Thus, by using commercially available off-the-shelf optical components a research grade optical imager has been developed. These imagers performed successfully during vapour cloud release experiment conducted on 15 January 2010.*

2. Scientific background

Upper atmosphere is a highly coupled system as it contains both neutrals and plasma in the same volume. There are dynamical processes in the upper atmosphere which depend on differential heating of the region by solar radiation. Neutral winds refer to the movement of the uncharged (neutral) species of the atmosphere, while the movements of charged particles are referred to as plasma drifts. The momentum and energy source in this region comes from the dissipation of tides, planetary waves and gravity waves that propagate upwards from the troposphere. These parameters are known to modify the structure of the ionosphere as well. Waves of different scale sizes and strong winds contribute to the transport of energy and momentum, both horizontally and vertically, in space. On some occasions these waves and winds, in part, contribute to the generation of plasma instabilities which produce variations in the refractive index of the medium resulting in phase and amplitude fluctuations of the radio waves propagating through this region. This phenomenon produces scintillation of the radio signals in the medium and contributes to disruption of long-wave trans-ionospheric radio communication from the satellite to different points on the ground. Therefore, it is utmost important to understand the dynamical variations in the upper atmosphere. There are several means by which the plasma drifts can be measured by employing radio techniques. However, it is extremely difficult to measure the neutral winds in the upper atmosphere. Methods to derive neutral winds do exist, some of them are briefly described below:

- **Radar tracking of meteor trails:** Meteor trails serve as tracers for the neutral winds. When a meteor ablates in the earth's upper atmosphere, part of the dissipated energy goes into ionizing the air in a column around the meteor. These trails are formed in the height range of 80-110 km and their motions can be tracked by a meteor radar. In this altitude region, as the ion-neutral collision frequency ν_i, is greater than the ion gyrofrequency ω_i, ($\nu_i > \omega_i$) the motion of this ion trail as investigated by the meteor radar represents the magnitude of the neutral wind.
- **Doppler shift of natural airglow emissions:** There are regions in the upper atmosphere where atomic and molecular constituents produce chemiluminescent emissions. Especially atomic oxygen emissions undergo Doppler shift as they move with the neutral wind. High spectral resolution measurements of oxygen emission line profile like Fabry-Perot interferometers provide a possibility of obtaining Doppler shifts and thereby enable information on the neutral winds at the altitude of origin of the emissions. For O (^{1}D) 630.0 nm emission the wind magnitudes that can be derived from this technique correspond to the altitude range of 250-300 km.
- **Incoherent scatter radars:** Incoherent scatter radars work differently from the conventional radars. The incoherent scatter echo is due to Thompson scattering of electrons that are in random thermal motion in the ionosphere. Therefore, the echo received by the radar will not be at a single frequency, but at a range of frequencies centered around the transmitted frequency. Due to the electrical interactions between the ions and electrons, the width of the spectrum provides information on the ion temperature. The observed spectrum usually has two peaks, and the height of these peaks dependent on the electron temperature. In addition to the electron and ion thermal motions, the entire plasma is usually in motion forming a plasma wind. As a result, the entire spectrum will be shifted instead of being centered on the transmitter frequency. By measuring this shift, and after the consideration of the magnetic field line geometry and ion-neutral interaction in the region, wind speed can be derived from the spectrum. A recent work (Santos et. al., 2011) compared the long term trends in the upper atmospheric neutral winds over Arecibo, Puerto Rico using this and the Doppler shift techniques.
- **Radar tracking of chaffs released by rockets:** A cloud of small strips of metals, such as copper or aluminum, which are cut to half the wavelength size of that corresponding to a given frequency of the tracking radar are released at high altitudes (<95 km) from a rocket. These metallic pieces, also known as window dipole, foil cloud, or foil chaffs, are blown by the ambient neutral wind as they fall to ground due to gravity. These chaffs act as a diffusive radar target and are tracked by the ground-based radar. The magnitude and direction of wind velocity at different altitudes in the middle atmosphere are computed from the range and angle data obtained by the tracking radar. The radar measures position coordinates of the chaff (R, θ, φ) as a function of time, where R, θ and φ are the range, elevation, and azimuth angles, respectively. This method can be used up to an altitude of 95 km to derive information on the altitude profile of the wind velocity (Widdel, 1985 and references therein).

- **Optical imaging of rocket released chemical vapours:** The technique of chemical vapour release from sounding rockets has been employed for measuring neutral wind and electric field in the mesosphere lower thermosphere region. Some of the chemicals used in the payloads are Sodium (Na), Lithium (Li), Trimethyl Aluminium (TMA) and Barium-Strontium (Ba-Sr). The chemical vapour released from the rocket serves as a reference point for triangulation so that wind velocities as a function of height can be determined from the photographs of these visible clouds taken from different locations on the ground.

- *In-situ* measurements of neutral winds have been made from the Dynamic Explorer (DE-2) satellite by using a quadrupole mass spectrometer. This spectrometer, called the Wind and Temperature Spectrometer (WATS) (Spencer et. al., 1973), measured the zonal and vertical components of neutral winds and also the kinetic temperature of the gas. In this technique, quadrupole mass spectrometer tuned to N_2, was coupled to the atmosphere through a precisely orificed antechamber with two scanning baffles in front of the orifice. One baffle moved vertically and the other moved horizontally. The angle of arrival of the gas stream with respect to the spacecraft is measured precisely by the instrument. With information on this angle and the known orientation and velocity of the spacecraft, zonal and vertical components of winds were calculated. Also, from the variation of N_2 densities, as the baffle swept past the orifice, kinetic temperatures were calculated.

In the past, the chemical release technique was used to derive neutral winds, diffusion and temperature in the altitude region of 80-400 km. Since 1955 many chemical release experiments have been carried out to measure these parameters in the upper atmosphere. After being released from the rocket the chemical vapour moves with the ambient wind. To measure winds and diffusion profile with height the vapour cloud is photographed by ground based cameras for over a period of several minutes. These photographs are analyzed by the method of triangulation (briefly described in section 3) to infer the motion of the trails. Sodium trails are visible due to resonant scattering of sunlight at wavelengths of 5890 and 5896 Å; similarly Lithium trails are visible due to red-light resonant scattering at 6708 Å. As these gases provide resonantly scattered light, these trails are extinguished quickly after sunset. Therefore, wind measurements using Na and/or Li as a tracer can be made only at dusk or dawn when the trails are illuminated by the sunlight but the observing sites on the ground are in the earth's shadow. On the other hand, TMA reacts with the atmospheric oxygen to produce chemiluminescence, resulting in a broad continuum emission. When illuminated by the sun, these trails produce an additional resonant emission with a peak intensity at 4842 Å. Therefore, TMA can be used even during nighttime. To derive neutral winds and electric fields for regions higher than 150 km, Barium-Strontium vapour blobs are used. A mixture of Ba and CuO (oxidizer), with an excess of Ba is evaporated, resulting in vaporized Barium. Strontium is always present as an impurity in the Ba metal. The neutral Ba vapour in the ionosphere resonantly scatters the solar radiation at 5535 Å. Above 150 km barium vapour gets ionized by solar UV radiation, and it scatters light with a peak wavelength of 4554 Å. On the other hand, Strontium remains unionized throughout and thus, moves with the neutral motion. Its motion can be traced as it gives a visible (4607 Å) emissions. The barium release experiment can be carried out only during twilight time as the ionization of barium vapour is not possible in the absence of direct solar radiation. As the motion of the ion cloud is dictated by the ambient electric and magnetic fields while that of the neutral strontium by the ambient neutral winds, the ion and neutral clouds get separated soon after the release. Therefore, by the method of triangulation it is possible to determine both the ion-drift and neutral wind velocities. Although vertical winds are much smaller in magnitude than the horizontal ones, spherical cloud/blob/point-release techniques are used for making those measurements.

3. Analysis method using triangulation technique

Triangulation refers to the process of determining the location of a target based on measurements from two known locations. In this method, the distance between the two stations from where the photographs are taken is known. The angles to the target from these two stations are calculated from the photographs taking the background star field as the reference. Based on these inputs, it is then possible to construct a triangle to determine the absolute location of the target. The method of triangulation is schematically represented in figure 1. The vapour trail is photographed from two camera stations S_1 and S_2 whose position vectors, r_1 and r_2 with respect to the rocket launch pad (A) are known. C_1 and C_2 are points on the cloud identified from the photographs taken from the two stations S_1 and S_2, respectively. Ideally C_1 and C_2 should be same. Vectors representing the lines of sight of the point C_1 and C_2 are $\mathbf{R}_1$ and $\mathbf{R}_2$, respectively. The direction cosine of the vector $\mathbf{R}_1$ and $\mathbf{R}_2$ are

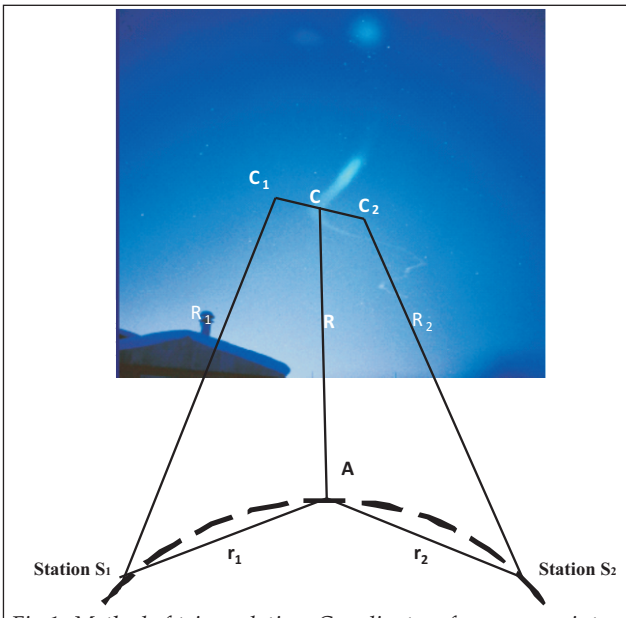

Fig.1: Method of triangulation: Coordinates of common points on the vapour trail are found from two or more stations. The movement of this point with time gives information on the horizontal wind speeds at that altitude (adapted from B. G. Anandarao, 1977, Ph.D. thesis).

known but their magnitudes are not known. Using trigonometry we can find out vector **R** for every set of two photographic frames from the two stations. Once **R** is known at different times the velocity components in x, y, z directions can be obtained from the positions at different times, and thereby the information on the magnitude of ambient winds could be derived.

Identification of common points on the cloud in the photographs taken from different stations is very crucial. In the case of blob releases the cloud is either spherical or ellipsoidal (if wind shears are prominent), and so its center can be easily identified from the photograph. However, in the case of a trail release, identification of common points is very difficult. Line-of-sight projection method is used to find the common point on the cloud as seen from two different stations. The line-of-sight in an image is a line that passes through the camera's center of projection and extends to infinity. When projected onto the image, the entire line appears as a single point. Instead, if the line-of-sight is projected onto another camera pointed at the same feature, it does not appear as a single point, but rather, as a line. This occurs because the line does not pass through the second camera's center of projection. The point of intersection of this line with the trail gives the corresponding point on the trail. To translate such points into inferring atmospheric parameters, such as winds, it is required that the photographic image is scaled properly to spatial distances in the sky. This is done by matching the stars photographed in the image to that in the stellar atlas. By doing this, the plate scale of the image is obtained based on which the coordinates of the image can be transferred to astronomical coordinates.

In the case of digital images or scanned negatives, the plate coordinates/plate scale of an arbitrary pixel can be determined from the knowledge of the camera's field-of-view (FOV), frame size and the resolution of the digital image. Plate coordinates are measured in pixels or millimeters. By doing such a scaling, the look-angles and the intersections of the lines-of-sight of the trail from two or more sites can be estimated so as to determine the trail position in the sky at a given time. The above information as a function of time enables estimation of the ambient wind speeds.

4. Film based techniques used earlier

In order to appreciate the optical imaging technique being currently discussed, it is useful to draw attention to the techniques employed earlier. The success of optical imaging of the chemical release depends upon both the brightness of the source and the contrast between the source and the background. Optical imaging most commonly involves cameras, either film or electronic detectors. Earlier experiments carried out in PRL and elsewhere used film cameras (e.g. Kodak K-24 and Hasselblad cameras). The vapour trails were generally photographed by using K-24 cameras equipped with 175 mm f/2.5 lens that used to image the scene onto a 5″x5″ film format and had a FOV of 23^0x23^0. The gap between two successive frames is ~2 inches. Typically, a maximum of one, 50 feet long roll can be loaded in the magazine which yields a usable exposure for about 80 frames. The power required by the camera for winding the film is ~360 Watts with 15A at 24 volts, and therefore, heavy duty batteries are required to operate the camera. On the glass plate, which keeps the film in position, a fiduciary marker was used to serve as the reference point on the film. An additional electronic circuit was used to synchronize the operation of the fiducial lamp and the timing of film exposures. Different films were used to photograph different chemical releases depending on the spectral-sensitivity of the film. For example, KODAK 2498 or TRI-X films were used to photograph Sodium, Barium, Strontium, and TMA clouds. Since these films were not red-sensitive they cannot be used to photograph Lithium clouds (Li emission line wavelength is 6708 Å). For Lithium emission measurements, KODAK 2485 70 mm film, which is more sensitive to red light, was used. To ensure the visibility of sufficient stars to provide information of the plate scale, high speed film (typically 1600 ASA) and long exposure times (~20-30 seconds) were used.

Fig.2: Hasselblad and K-24 cameras mounted on tripods.

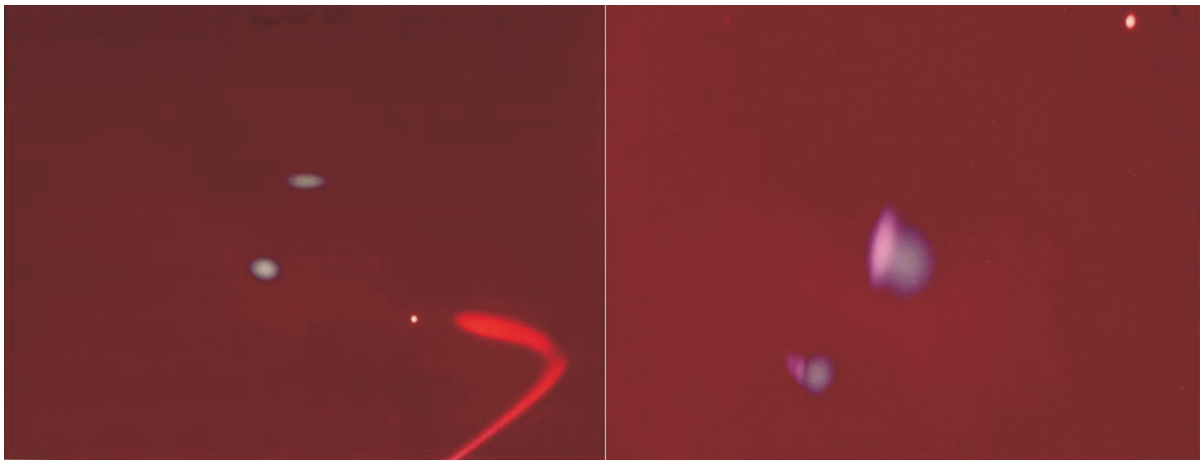

(a) (b)

Fig.3: (a) Barium blob releases at altitudes of 137 and 150 km during upward leg and Lithium trail release which started from 132 km during downward leg of the Centaur rocket. (Launched from Thumba on 16 February 1980 at T_0=18:55 IST. This photograph was taken at T_0+755 seconds). (b) Barium blob released at altitudes of 183, 228 and 308 km. Rocket was launched from SHAR on 16 February 1982 at T_0 = 18:43:14 IST. This photograph was taken at T_0+305 seconds after the release of fifth blob. Third blob was released at T_0+123 sec. As can be seen from the figure Barium cloud is aligned with the magnetic field lines and Strontium which remains unionized is seen as a blob (R. Sekar, 1990, Ph.D. Thesis).

HF radio communications for remote locations or telephone lines (if available) were used to communicate between the rocket launch station and different field stations. For time synchronization, stop watches were used that were be adjusted to the rocket range time just before the rocket launch. In order to ensure uniform exposure times, a predetermined exposure schedule was used at all the camera sites. Two different types of cameras that were used by PRL scientists in the earlier years to photograph vapour cloud are shown in figure 2.

Before the analysis of the data can be carried out, these films are first required to be developed and its plate coordinates were to be read by using a travelling microscope. The right ascension (RA) and declination (DEC) values of the stars on the photographs were obtained from the star atlas. Possible sources of errors in this experiment are; (1) incorrect determination of the latitude and longitude of the camera position, (2) error in identifying the stars and in reading their coordinates, (3) error in drawing the central line on the vapour trail image, and (4) limited accuracy of the microscope. To reduce these errors, timing and height information of the released cloud needs to be accurately determined.

PRL had done pioneering work in studies related to deriving neutral upper atmospheric winds, turbulence, temperature, density and interaction of the neutral and ionized upper atmosphere through rocket-released chemical vapour cloud technique. This work started in PRL as early as 1963 by P D Bhavsar and Ramanuja Rao (K. Ramanuja Rao, Ph.D. Thesis, 1966) with the sodium vapour release experiments at twilight hours for neutral wind measurements. In fact, the first rocket that left the Indian shore was carrying a vapour release payload. Later, TMA release technique was applied during night hours also (M.S Narayanan Ph.D. Thesis, 1973). Vertical winds in the 90-200 km range were studied by Barium-Strontium cloud release during twilight time (Raghavarao et. al., 1984). Daytime wind measurements were attempted by using differential photometric technique to track Lithium vapour clouds released in upper atmosphere. Electric fields were measured by Barium cloud experiments over the dip equator (Thumba). The photograph of Barium blob and Lithium trail released simultaneously is shown in figure 3(a), Barium-Strontium blob released at different altitudes is shown in figure 3(b). The effects of horizontal winds and the vertical shear in the meridional and zonal wind components on the equatorial electrojet parameters (like current intensity, width and thickness) were quantitatively studied (for e.g. B. G Anandarao, Ph.D. thesis, 1977, Raghavarao and Anandarao, 1980).

One of the last vapour cloud release experiment from India was carried out for F-region studies during the ionization-hole campaign in 1993. In this campaign, multiple instruments were used to study the F-region neutral and electrodynamics to understand the background ionospheric and thermospheric conditions at the onset of the equatorial spread-F. One of the major experiments in that campaign was Barium-Strontium release from the rocket which provided all the three components of the winds and the ambient electric fields (Sridharan et. al., 1997).

5. Development of highly sensitive digital camera system for imaging rocket released vapour cloud

This section gives a detailed account on the development of highly sensitive digital camera system. As will be shown, such digital imagers are well suited for field experiments, especially for challenging experiments, such as, rocket released vapour cloud photography.

With electronic imagers, it is found that contrasts even as low as 5%-10% permit useful observation of light from the chemical release against the sky background as opposed to the high speed film based cameras which require a contrast of at least 20% (Neil Davis, 1979). The typical exposure time for a

Hasselblad camera for photography of TMA vapour cloud during twilight even with high speed films is ∼20 sec in comparison to ∼5 sec exposure of a digital single lens reflex (SLR) camera (Ingersoll, 2008), for the same optics. With new technological advancements in digital imaging sensors, the digital SLRs are capable of giving comparable or better spatial resolution than the film cameras. The better resolution and higher contrast in digital imaging improves the accuracy of the position information for the vapour cloud released (as described in section 3) and hence reduces errors in the estimation of winds.

To photograph the vapour cloud a sensitive camera along with a filter (centered on the wavelength of scattering of the chemical release) and an objective lens that defines the FOV are required. The present day technology provides high sensitive and large dynamic range electronic array detectors that use active pixel sensor technology. Digital SLR provides flexibility in choosing FOV by using different objective lenses in the front-end and an option of placing a filter in front of the lens. Further, theses cameras can also be easily automated for carrying out synchronous photographic operations thereby ensuring highly accurate time and space information of the cloud. By using digital imaging methods, the subjectivity in the analysis is minimized which increases the reliability of thefinal result. Due to a large dynamic range and a wide spectral response of the digital detectors, these cameras can be used for releases of different chemicals which resonantly scatter/emit at different wavelengths. To operate these cameras one requires only a laptop, and therefore, once the batteries of the cameras and the laptop are charged, they can be operated without any stringent power requirement -even during the actual experiment in the field.

The commercial digital cameras have been augmented with high quality optical filters and lenses to make them science grade imagers meant for scientific research. These imaging systems are rugged, portable, easy to operate, less expensive, and more reliable when compared to the earlier cameras that were used for photography of rocket vapour trail. The different critical components of the imaging system are described below.

5.1. Digital cameras

For the present work we have used commercially available Canon digital SLR camera (Canon EOS 50D). These cameras need to be run in an automated manner so that any change required for camera settings can be carried out through the specially developed camera control software. The specifications of the camera are given in table 1:

Specification of digital camera	
Type	Digital Single Lens Reflex (DSLR), 15.1 megapixels
Sensor	Single plate CMOS sensor, Size 22.3 x 14.9 mm (Aspect ratio 3:2)
Image type	RAW (14-bit, Canon original), JPEG, sRAW, RAW+JPEG
Exposure control	ISO 100-3200, flexibility in setting aperture size and exposure time
Shutter	Vertical-travel, mechanical, electronically-controlled, focal- plane shutter, speed range 1/8000 to 30 sec.
Interface	USB 2.0 for PC communication
Battery	One Battery Pack BP-511A, AC power can be supplied via optional AC Adapter Kit ACK-E2
Dimensions and Weight	145.5 x 107.8 x 73.5mm, 730g (body only)
Working temperature and humidity range	0-40°C, 85% or less
Lenses	Canon EF lenses, (35mm-equivalent focal length is approx. 1.6x the lens focal length)

Table 1: Technical specifications of canon EOS 50 D camera

5.2. Choice of the objective lens

The choice of an objective lens is governed by the parameters such as diffusion, winds etc. that one needs to measure. Therefore, the FOV is decided by the altitude range of the vapour trail release, distance of the camera station from the rocket launch site, an estimate on the movement of the vapour cloud released, and the desired altitude resolution. To photograph the vapour cloud released, it should ideally be in the middle of the FOV of the camera and it should remain in the FOV till the end of the experiment. Therefore, the choice of the objective lens, which defines the FOV, is an important parameter. Most of the digital SLR cameras have image sensors which are smaller than the full frame 35 mm film cameras. Conventional film cameras have an image area of 24 x 36 mm (diagonal 43.3 mm). Digital SLR cameras usually use the same lenses that are made for the standard 35 mm format film cameras. The focusing lenses still focus the image onto the same plane as before, but as the sensors are smaller in size than the 35 mm format films, the entire image is not captured by the digital SLR cameras for the same focal length of the lens. Thus, smaller sensor size in digital SLR cameras results in a cropped FOV. Therefore, in DSLRs this crop factor/ focal length multiplier (FLM)/ format factor is required to be taken into account. This is defined as:

$$\text{Crop factor/FLM} = \frac{\text{Diagonal of 35mm film (43.3mm)}}{\text{Diagnol of the sensor in question}} \quad (1)$$

For example, for a canon 50 D camera whose sensor size is 22.3mm x 14.9mm and a diagonal of 26.8 mm will have a crop factor of 1.6. Therefore, the product of the focal length of the lens and the crop factor gives the focal length of a lens that would yield the same FOV if it were to be used in the standard 35 mm film camera.

The camera FOV is given by:

$\alpha = 2*\tan^{-1}\frac{s}{2f}$, which can be approximated to $\alpha = \frac{180s}{\pi f}$ degrees. (2)

where,

s = size of the sensor (length, breadth or diagonal) and f = focal length of the lens The angle of views for a Canon 50D cameras focused at infinity is given in table 2.

Focal length of the lens (mm)	Horizontal (α_h) (degrees)	Vertical (α_v) (degrees)	Diagonal (α_d) (degrees)
50	25.6	17	30.7
35	36.5	24.4	43.9

Table 2 : Angle of view for a Canon 50D camera

5.3. Sensitivity estimation of digital camera sensors

The DSLRs contain electronic sensors which are either complementary metal-oxide semiconductor (CMOS) (for e.g. Canon) or charge-coupled device (CCD) (for e.g. Nikon). The basic difference between the two sensors is in the way the electrons generated by photons in the semiconductor material are read out. In CCD the electrons are shifted from pixel to pixel one by one until they arrive at the output, then the voltage is amplified, digitized, and sent to the computer. However, in the CMOS sensor each pixel has its own small amplifier, along with row-by-column connections so that each pixel can be read out individually and there is a main amplifier along with other control circuitry at the output. Each pixel in the sensor can hold finite number of electrons that are generated from the photons falling on the sensor and this is called the full-well capacity, which is a function of the pixel area and the bit value of the detector. Canon 50D camera sensor details are given below in table 3:

Full well capacity	27300
Pixel size	4.7 micron
Data coding	14-bit
Inverse electronic gain @ ISO 400	0.57 electron/ADU (analog-to-digital units)
Readout noise @ ISO 400	8.56 ADU (4.9 electrons)
Bias level	1024 ADU
Thermal signal @ 22^0 C	0.06 electron/sec
Full wave capacity @ ISO 400	8700 electrons
Dynamic range @ ISO 400	full well capacity/readout noise =8700/4.9=1770

Table 3: Sensor details of the Canon 50D camera

To calculate the sensitivity of the detector let us assume that a source that extends 1 square arc second in the sky, emits 100 photons/second.

Angle subtended by a pixel is:

$\alpha = \frac{180d}{\pi f}$ degrees = 206265 x d/f arc seconds,

where *f* is the focal length of the lens and *d* is the width of the pixel.

For f=50 mm and d = 4.7 microns,

$\alpha = 206265 \times 4.7*10^{-3}/50 = 19.39$ arc seconds

For color coding, the sensor uses Bayer organization in which 2x2 color filter array (CFA) elementary structure is used. In this structure we have 1 pixel for red channel, 1 pixel for blue channel, and 2 pixels for green channel. Therefore, for Bayer configuration quantum efficiency is reduced by a factor of 0.25, 0.25, and 0.50 for red, blue and green spectral bands, respectively.

For basis CFA structure (2x2 pixels) angle on the sky would be $\{(2x2) \times (\alpha x \alpha)\}$.

The number of photons received per second in the cell of CFA = 4 x 19.39x19.39x100 =150400 photons

Considering an efficiency of 20% for a given wavelength which includes the efficiency of CFA mentioned above, (quantum efficiency varies as a function of wavelength, which is 2-20% for EOS 50D camera sensor). Therefore, the number of photoelectrons formed are = 150400x0.2= 30080 electrons.

For a 14-bit detector, these number of electrons are sufficient enough to be detected.

5.4. Filters

To increase the contrast of the photograph, a filter is used in front of the lens. The mounting of the filters can be easily done in the canon EF lenses because of an additional slot that is provided in front of the lens. With the help of additional adapter the filter was arrested on the camera lens.

When TMA is released in sunlight a blue resonance spectrum is found, which is superimposed on the continuum of the chemiluminous glow in the range of 4500-5500 Å. The photograph of the chemical trail taken during twilight time is shown in figure 4.

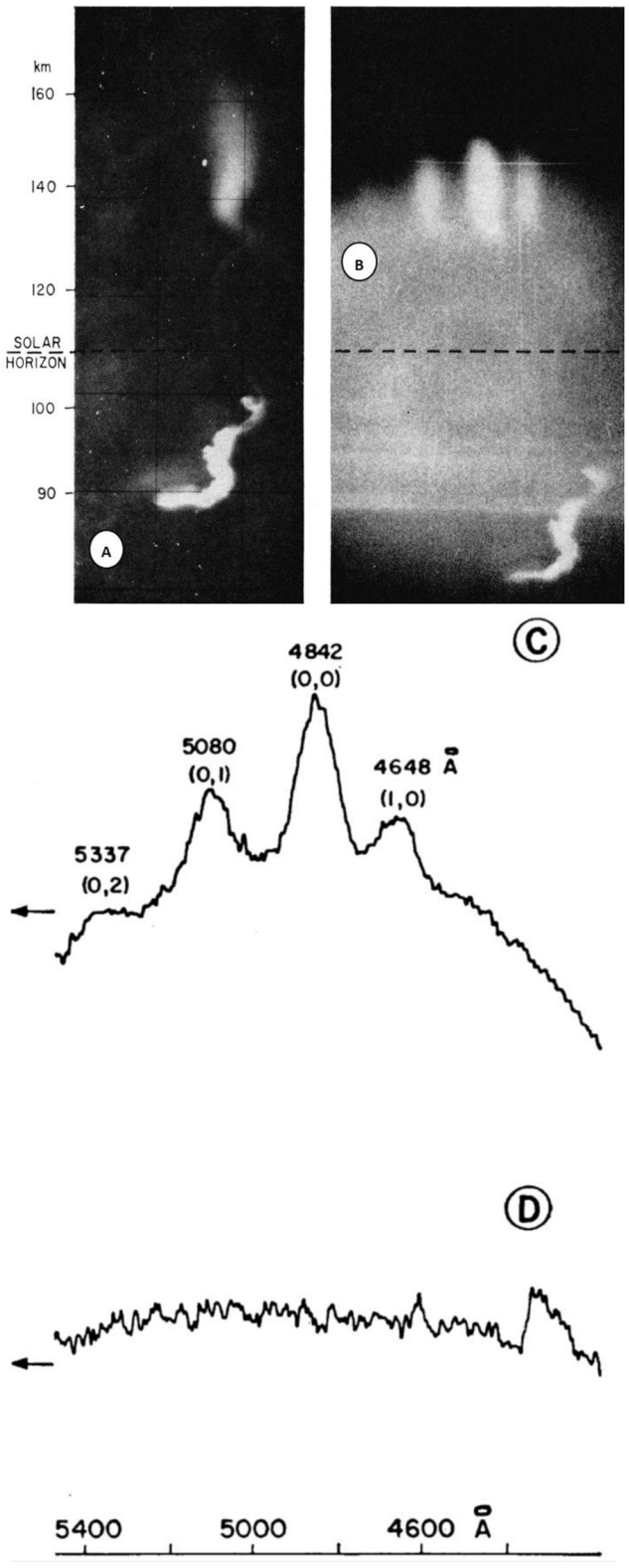

Fig.4: (A) photograph taken with an ordinary camera during twilight (exposure time 5 sec) (B) photo taken with a camera equipped with a transmission grating to spread the image into its spectral components which shows four spectrally separated images of the upper (sunlit) portion of the trail, where emission is largely in four Aluminium Oxide (AlO) resonance bands. The non-sunlit portion of the trail in the lower portion of the image shows only a continuum (chemiluminous) emission. C and D are densitometer traces of upper and lower parts of photo B, with a wavelength scale shown below (After Rosenberg et.al., 1964).

In the presence of sunlight the aluminum oxides in TMA released is also capable of resonantly scattering the sunlight, which gives rise to a band spectrum with a maximum intensity at ~4842 Å (bluish green). To capture these emissions a 2 inch (50.8 mm) diameter broadband optical glass filter with a peak transmission > 90% in the wavelength range of 4200-5200 Å with central wavelength at 4700 Å and a bandwidth ≤ 1100 Å was used. The filter wavelength and transmission were calibrated at PRL, and the calibration curve is given in figure 5.

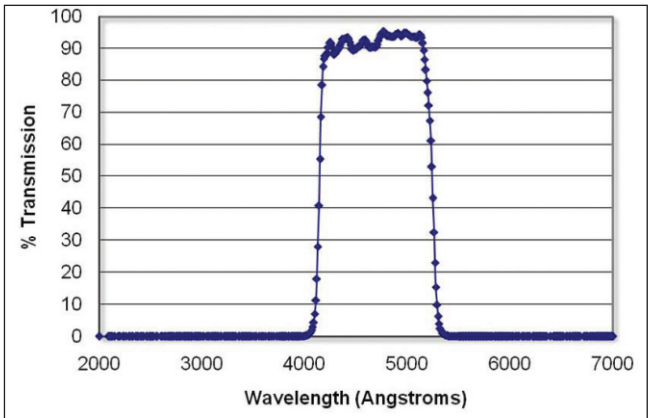

Fig.5: Filter transmission curve measured at PRL.

5.5 Estimation of signal-to-noise ratio

This section presents a detailed discussion on the estimation of signal-to-noise ratio (SNR) of measurements made by the digital imagers that are discussed in this report. The SNR critically depends not only on the signal brightness, but also on the background intensity level, readout noise, dark noise, and the efficiencies of various optical components used in the system. For making such an estimate of the SNR, all the required parameters as detailed in the CEDAR tutorial (on "Errors in Airglow & Auroral Emission Measurements") by D. Pallamraju, 2003 are considered and are given below.

$$\frac{S}{N} = \frac{S}{\sqrt{(S+B)+D+R}} = \frac{qe \bullet s \bullet ft \bullet t \bullet k \bullet ke}{\sqrt{[qe(s \bullet ft + bg \bullet fa)\, t \bullet k \bullet se + d \bullet t + (ro)^2]}} \quad (3)$$

where,

S is signal, B is background D is dark noise or thermal noise of the detector, R is read out noise of the detector.

qe = detector quantum efficiency =0.05 (taken for 6708 Å Lithium line)

s = signal strength = 0.5 MR (taken for 6708 Å Lithium line, B. G. Anandarao, Ph.D. thesis)

ft = filter transmission = 0.94 (assuming a similar transmission for 6708 Å as in figure 5)

t = exposure time = 10 seconds (used for the image shown in figure 8)

bg = background transmission = 1 RÅ^{-1} (nighttime background, Pallamraju, CEDAR tutorial, 2003)

fa = filter bandwidth where background is considered =1100Å (see figure 5)

d = Dark noise = 0.06 e$^-$ pix^{-1} s^{-1} (see Table 3)

ro = readout noise = 4.9 e$^-$ (RMS) (see Table 3)

k = photons s^{-1} R^{-1} pixel^{-1} incident on a pixel of given area and given f/#

se = system efficiency (considered as equal to 1)

For nighttime photography, as obtained by the digital camera being discussed in this report (and shown in figure 8), exposure time is 10 seconds for f/2 lens, Diameter of the lens, D=50.4 mm, focal length of the lens, f = 100.08 mm, pixel size of the detector used in canon EOS 50 D, s = 4.7 microns.

Considering all these values, we get,

$k = (10^6/4\pi) * \pi (D/2)^2 * (s^2/f^2) = 3.45 * 10^{-3}$ photons $s^{-1} R^{-1}$ pixel^{-1}

S = 810.75 photons pixel^{-1}

B = 1.89 photons pixel^{-1}

D = 0.6 e^- pixel^{-1}

R = 24.01

$$SNR = \frac{S}{\sqrt{(S+B)+D+R}} = 28.04 \quad (4)$$

Therefore, signal-to-noise ratio for such a measurement made by the digital imagers turns out to be 28.04, which is a clear and unambiguous measurement as the uncertainty (1/SNR) of such a measurement is just 3.57 %.

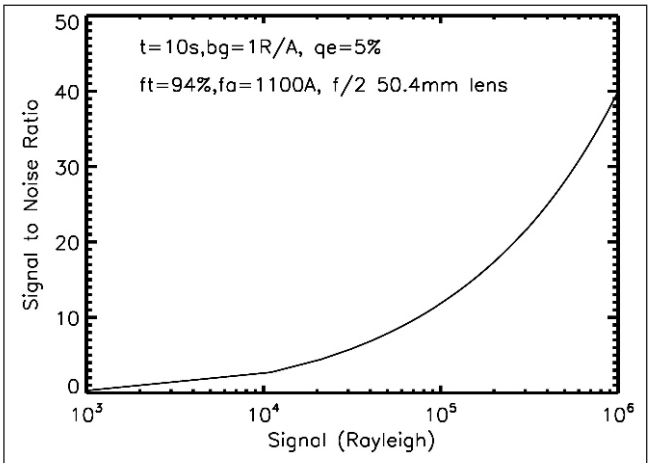

Fig.6: Log-linear plot of signal vs SNR, all other parameters in equation 3 are kept constant.

The signal strength of the released vapour cloud depends on many factors, such as, quantity of the chemical released, location of the camera stations, diffusion at a given altitude, phase of the cloud release. As the signal strength varies with these factors, an estimate has been made on the SNR for different signal strengths and the results are shown in figure 6. One can note that SNR is >1 for a signal of ~2200 R for an exposure time of 10 seconds. Estimates, as shown in figure 6, will be useful in deciding the amount of chemical to be released so that it produces the required signal.

6. Software requirements

As mentioned earlier, for imaging of vapour trail released by rocket, it is extremely essential that the operations of digital imagers be synchronized. Such a work was carried out by using "DSLR remote Pro multi camera" software which allows multiple Canon EOS DSLR cameras that are interfaced through USB to be operated from a single PC. After connecting cameras to the computer through USB the camera controls remain fully operational and the camera settings can be carried out both by using the knobs on the camera and by software driven interface. Similarly, the photographs can also be taken manually by using the camera's shutter release mechanism or remotely from the PC.

For redundancy, and also to cover the vapour trail in different plate scales to enable better estimation of diffusion/winds it is required that at least two cameras be operated at a given station with two different FOVs. Following requirements are implemented in the software:

6.1. Camera configuration

Different settings of the camera are: aperture size, exposure time, ISO, size/quality of the image, start and stop time, etc. One needs to connect the two DSLR cameras through the software such that all the operations on the camera, as mentioned above, can be carried out by using only the software and without any manual intervention.

6.2. Image acquisition and storage

The time at which an image is obtained is very important for the data analysis. Before the camera's start taking images, the clocks of all the computers located in different stations are to be synchronized. The cameras then start taking images as per the settings enabled through the software. These images are stored in the computer and the names of the images are programmed such that they contain the time information in the HHMMSS format.

The different camera settings that can be carried out through the software are shown in the snapshot (figure 7). The different settings implemented in this software are:

- The frame on the left shows the camera setting in which different parameters for the camera, such as aperture size, exposure time, ISO, image quality, can be set.
- The middle frame shows image storage setting in which the name of image is given in HHMMSS format and the directory in which the images are to be stored can be set.
- The frame on the right shows setting for the time lapse photography in which the start and stop time for photography can be set. The time interval between two images can also be set.

7. Advantage of digital imaging over film based imaging

The uncertainty involved in the triangulation technique depends on the star fit and the accuracy with which the points on the chemical release are identified. In the film based photography, the film is first developed and after carrying out photo-densitometry analysis the brightest point on the image is marked manually. These images represent line-of-sight integrated brightness and therefore the appearance of the cloud in the image is sensitive to the angle of the line-of-sight. Therefore, improper identification of the same point from two stations leads to an ambiguity in the data analysis. It is known that the major source of error in the data analysis is in the drawing of the central line of the trail. Identification of the common point in film based photography is quite an involved process. In the case of digital imaging, firstly the uncertainties due to the human errors can be reduced as the markings of central brightness can be achieved by employing image

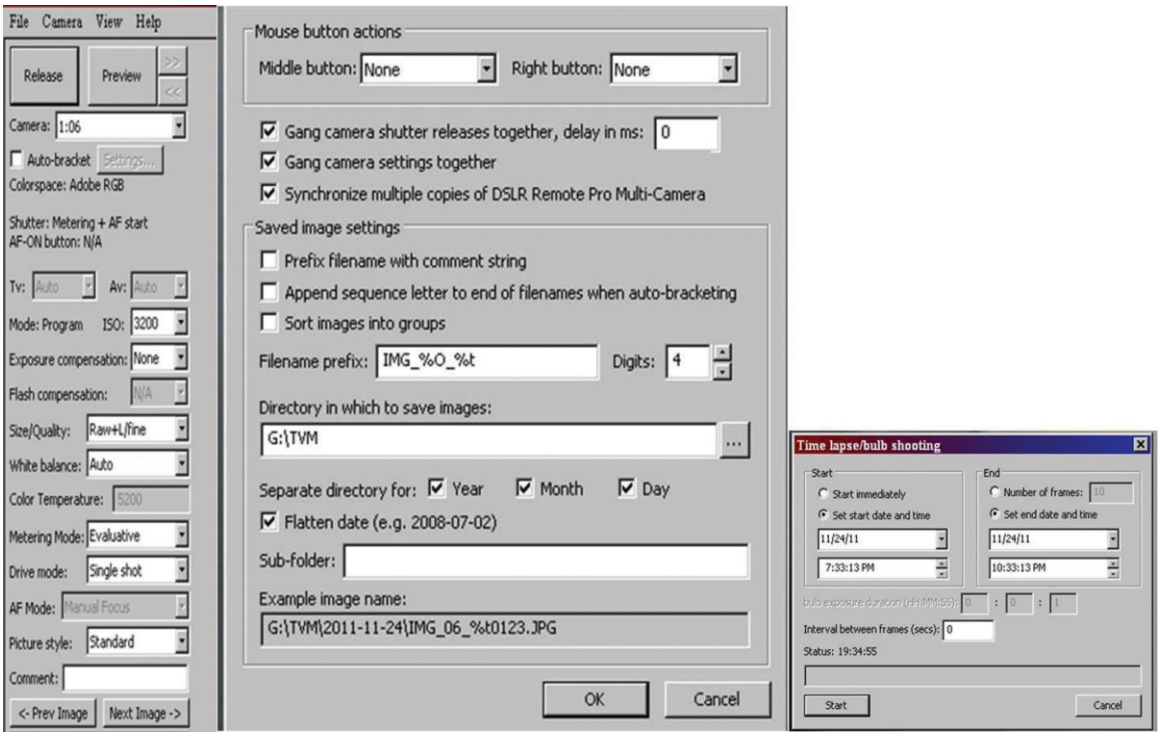

*Fig.7: S*napshot of the software windows showing different camera settings.

optimization and Fourier analysis techniques on the digital image obtained. This information can directly be given as an input to the program to accurately calculate the position of the blob in all the three coordinates as a function of time. Secondly, the repeatability of data analysis can be checked on digital images in order to reduce uncertainties and to verify the results by employing different analysis approaches. Thirdly, by using digital images the total time taken in the data analysis reduces considerably. Further, imaging of different vapour clouds released that emits at multiple wavelengths can be carried out by a single imager just by changing the filter. Furthermore, the ease of carrying the cameras, their installations in the field station, the logistic support (in terms of power requirement, operation etc.) are minimal when compared with the bulky and heavier equipments employed earlier.

For the purpose of comparison, a first order calculation to derive the uncertainty in the position measurement of the vapour clouds has been done for both digital photography and for film based photography.

In the digital image, the minimum uncertainty of fixing the point is generally of the order of 1 pixel. With 25.6^0 x 17^0 FOV (for a 50 mm objective lens) the uncertainty in the angle measurement by using the digital camera with 4752 x 3168 pixel resolution is $25.6^0/4752 = 5.39 \times 10^{-3}$ degrees. Assume the trail point is at a height of 110 km, the uncertainty in position measurement in the vapour cloud is 110 x tan (5.39×10^{-3}) = 10.34 meters. In the film photograph, the points are read by using a microscope. The uncertainty in fixing the point is of the order of 0.01 mm (least count of the microscope). Therefore, uncertainty in the angle measurement for same FOV (25.6^0) for a 5 inches format film is 25.6^0 / (5 x 25.4/0.01) = 2.015×10^{-3} degrees. Therefore, the uncertainty in position measurement in the vapour cloud at the height of 110 km by using 5 inch film format camera is 110 x tan $(2.015 * 10^{-3})$ = 3.87 meters. Similarly, for 70 mm film format camera uncertainty in the angle measurement for same FOV (25.6^0) is = 25.6^0 / (70/0.01) = 3.66×10^{-3} degrees. Therefore, the uncertainty in position measurement in the vapour cloud at the height of 110 km by using 70 mm film format camera is 110 x tan (3.66×10^{-3}) = 7.02 meters. It is apparent that the uncertainties in the position measurement are comparable in all the three situations as discussed above. Therefore, it can be seen that the digital imagers can be effectively used in the place of film based cameras as they provide us with several added advantages as mentioned earlier in this section.

8. Field experiment using this technique

The imaging technique mentioned above was conceived and realized in a short duration to carry out photography of vapour clouds released during the annular solar eclipse of 15 January 2010 on an exploratory basis. The vapour release technique is quite established to measure the neutral winds in the upper atmosphere as discussed in section 2. Until now this technique has been successfully used during night or twilight times. Some efforts were made earlier to measure daytime neutral winds in the upper atmosphere by using various other techniques, however, uncertainties involved in those measurements were large. The imaging of vapour cloud during annular solar eclipse was carried out to take advantage of the reduction in the sky brightness during the eclipse. A photograph of two cameras operating in a field station is shown in figure 8. The challenges to image the vapour release during the eclipse time and the innovative approaches that were followed to address a given issue are briefly described below:

- The daytime sky intensity is highly variable depending upon the spectral region and the position of the sun with respect to the location of observation. Typically the background radiance in terms of photon intensity is 3-5 x 10^{12} photons cm^{-2} sec^{-1} sr^{-1} $Å^{-1}$ (~3-5 MR/Å). For Lithium (6708 Å) vapour release the photon intensity is 5 x 10^{11} photons cm^{-2} sec^{-1} sr^{-1} (0.5 MR) (B. G. Anandarao, Ph.D. thesis and references therein). Therefore, the sky background intensity is about 10 times greater than that of the vapour trail. It was assumed that the scattered sky background intensity in the afternoon time (13:05 IST) during the eclipse could come down to such a value as mentioned above. *To photograph such a low contrast vapour cloud, a very sensitive camera in combination with a band pass filter was used so as to reduce the background brightness.*
- During nighttime/twilight time the vapour trail can be seen by naked eye. Therefore, the camera can be moved to focus the vapour cloud during the actual experiment. *Since the vapour trail cannot be seen by the naked eye during daytime, we have used two cameras per station with different FOV to ensure that the trail is covered. Knowing the coordinates of a given observational location, the azimuth, and elevation angles for a 90-100 km release of the TMA trail had been worked out and implemented. For an expected release of the TMA in the predefined altitudes, the FOV obtained by a 50 mm and a 35 mm focal length lenses as discussed earlier would suffice the requirement.*
- To obtain information of the plate scale, star photography at that RA & DEC is required. *However, as stars cannot be photographed in the daytime, the plate scale was obtained by carrying out the star photography in the nighttime without disturbing the camera positions and their orientations.*

Fig.8: Photograph of the imaging systems in a field station.

9. Implementation

To image the vapour trail, four different groups were made to carryout observations at four field stations around the rocket launching locations. The details of the stations from where the photography of the vapour trail was carried out are given in table 4.

Station name	Trivandrum	Kanyakumari	Tirunelveli	Amritapuri
Latitude	08^0 32′ N	08^0 04′ N	08^0 40′ N	09^0 05′ N
Longitude	76^0 52′ N	77^0 32′ N	77^0 49′ N	76^0 29′ N

Table 4: Field stations for vapour cloud photography.

A clear instruction manual was made and live demonstrations and rehearsals were carried out at PRL before the actual experiment. The laptops were synchronized with the NIST internet time server (time.nist.gov) a few days before the rocket launch. On the day of rocket launch the laptops were synchronized with the TERLS time. Therefore, all imaging systems in different locations were set to record the same time for each image in HHMMSS format. On the experiment day (15 January 2010) the annular solar eclipse occured close to Thumba with ~91% obscuration. The duration of eclipse was for 11 min 08 sec with the maximum obscuration occurring at 13:15 IST. A Rohini sounding rocket RH-300 MK-II carrying TMA and other experiments was launched at 13:05 IST from Thumba.

During the annular solar eclipse the 3 kg TMA that was released from the side of the rocket over a 23 km altitude did not produce sufficient contrast to discern the released vapour cloud. The cameras, however, performed flawlessly at all the four stations. As the observational tools are now in place, experiments are being planned for a nighttime TMA releases to both quantify the glow produced for a given quantity of TMA, and also to derive information on neutral wind fields. A typical photograph taken by the camera during night time is shown in figure 9.

To obtain a similar image, film based cameras would require exposure time of around 30 sec as can be seen in figure 3, it can also be seen clearly that the contrast of figure 9 is better than that of figure 3. If TMA is released in the nighttime (from the backend of the rocket to concentrate the TMA in one direction) which is much brighter than the starlight (as shown in figure 4), it can be easily photographed with better signal-to-noise ratio by using the imaging systems described in this report.

10. Summary

In this brief report the development of optical systems and their automation for photography of the vapour cloud released by a rocket to study upper atmospheric neutral winds is discussed. These systems are comparable in performance to the film based camera systems that were used earlier. Moreover, the ease of data analysis and repeatability using the data obtained by these digital cameras significantly reduces the subjectivity and considerable labour that exists with the analysis of photographs obtained by film based cameras. Further, the flexibility to use the same camera for photographing different vapour cloud releases that give signals at different wavelength is an added advantage. Thus, a research grade imaging system was realized by using off-the-shelf components. The digital imagers described in this report are rugged, reliable, portable, less expensive, easy to handle, install, and operate. These systems have been successfully tested in the field for actual operations.

Fig.9: Nighttime image of stars to obtain the plate scale. It can be noted that just for a 10 second exposure many stars are clearly seen (image was obtained on 15/01/2010 at 21:00 IST, solar declination angle was 20.98^0) as compared to figure 3 which was taken with an exposure time of 30 seconds (photo was taken on 16/02/1980 at 19:10 IST, solar declination angle was 12.34^0).

11. Acknowledgement

We would like to acknowledge the support and cooperation of several individuals, groups and institutions that have participated in various fronts. We thank Prof. B.G Anandarao and Mr. V. Venkataraman of Astronomy & Astrophysics division, PRL for enabling and assisting in carrying out filter calibration tests. We acknowledge the support of the Director, PRL for his support for carrying out this challenging experiment. We thank Dr. A. Rajendran and his team at VSSC, Trivandrum for preparing the canister and the TMA payload. We thank the project director, Mr. P. Ratnakar Rao and his team at ATVP/TERLS, VSSC for extending the required technical and logistic support for this experiment. We thank all the enthusiastic colleagues at PRL who participated in carrying out the imaging experiment at different field stations. We are thankful to the Heads and Directors of EGRL, IIG Tirunelveli, Amritapuri Engineering College Amritapuri, Kerala House, Kanyakumari, VSSC Trivandrum and their supporting staff for providing local hospitality and arranging logistics to carry out the experiments. We thank Profs. R. Sekar and R. Sridharan for carefully going through this article and making their critical comments which have significantly helped in increasing the clarity of this article. We thank reviewers for their constructive suggestions. The annular solar eclipse experiments were made possible under the auspices of the Climate and Weather of the Sun-Earth System (CAWSES-India) program sponsored by ISRO. In this regard, we would like to acknowledge the contribution of the CAWSES-India National Steering Committee and the support of ISRO in realizing this experiment. This work is supported by Department of Space, Government of India.

12. References

1. Anandarao, B. G., Studies on the dynamics of the equatorial Ionosphere, Ph.D. Thesis, Gujarat University, Ahmedabad, 1977.
2. Ingersoll J. E, A Regularization Technique for the Analysis of Photographic Data Used in Chemical Release Wind Measurements, Master thesis, Clemson University, 2008.
3. Narayanan, M. S., Studies in upper atmosphere, Ph.D. Thesis, Gujarat University, Ahmedabad, 1973.
4. Neil Davis, T., Chemical releases in the ionosphere, Reports on Progress in Physics, Vol. 42, 1565-1595, 1979.
5. Pallamraju, D., CEDAR Tutorial, 2003, Errors in Airglow & Auroral Emission Measurements, http://cedarweb.hao.ucar.edu/workshop/tutorials/2003/pallamraju03.pdf.
6. Rao, K. R., Studies in upper atmosphere "Measurement of neutral atmosphere winds above 80 km", Ph.D. Thesis, Gujarat University, Ahmedabad, 1966.
7. Raghavarao, R., and B. G. Anandarao, Vertical winds as a plausible cause for equatorial counter electrojet, Geophysical Research Letters, Vol. 7, 357-360, 1980.
8. Raghavarao, R., J. N. Desai, B.G. Anandarao, R. Narayanan, R. Sekar, Ranjan Gupta, V. V. Babu and V. Sudhakar, Evidence for a large scale electric field gradient at the onset of equatorial spread-F, Journal of Atmospheric and Terrestrial Physics, Vol. 46, 355-357, 1984.
9. Rosenberg, N. W., D. Golomb and E. F Allen Jr, Resonance Radiation of A1uminium Oxide from Trimethyl Aluminum Released into the Upper Atmosphere, Journal of Geophysical Research, Vol. 69, 1451–1454, 1964.
10. Santos P.T., C. G. M. Brum, C. A. Tepley, N. Aponte, S .A González, and E. Robles, Using incoherent scatter radar to investigate the neutral wind longterm trend over Arecibo, Journal of Geophysical Research, Vol. 116, 2011.

11. Sekar R., Plasma Instabilities and the dynamics of the equatorial F-region, Ph.D. Thesis, Gujarat University, Ahmedabad, 1990.
12. Spencer N. W., H. B Niemann, and G. R Carignan, The neutral-atmosphere temperature instrument, Radio Science, Vol. 8, 287-296, 1973.
13. Sridharan, R., H. Chandra, S. R. Das, R. Sekar, H. S. S. Sinha, D. PallamRaju, R. Narayanan, Shika Raizada, R. N. Misra, R. Raghavarao, G. D. Vyas, P. B. Rao, P. V. S. Ramarao, V. V. Somayajulu, V. V. Babu and A. D. Danilov, Ionization hole campaign- a coordinated rocket and ground-based study at the onset of equatorial spread-F: first results, Journal of Atmospheric and Solar-Terrestrial Physics, Vol. 59, 2051-2067, 1997.
14. Widdel, H.U, Foil clouds as a tool for measuring wind structure and irregularities in the lower thermosphere (92–50 km), Radio Science, Vol. 20, 803-812, 1985.
15. www.astrosurf.com
16. www.canon.co.in

PRL research encompasses the earth the sun immersed in the fields and radiations reaching from and to infinity, all that man's curiosity and intellect can reveal

पीआरएल के अनुसंधान क्षेत्र में समविष्ट हैं पृथ्वी एवं सूर्य जो निमीलित हैं चुंबकीय क्षेत्र एवं विकिरण में अनंत से अनंत तक जिन्हे प्रकट कर सकती है मानव की जिज्ञासा एवं विचारशक्ति